Collagen and Leather

RESEARCH

Open Access

Cartilage-like protein-polysaccharide hybrid hydrogel for enhancing chondrogenic differentiation of bone marrow mesenchymal stem cells

Xinyue Zhang[1,2,3], Xue Zhan[1,2], Haojin Cheng[1,2], Zuqin Dong[1,2], Chen Hu[1,2], Chenxin Liu[1,2], Jie Liang[1,2,4], Yafang Chen[1,2*], Yujiang Fan[1,2,3*] and Xingdong Zhang[1,2]

Abstract

The regeneration of articular cartilage posed a formidable challenge due to the restricted treatment efficacy of existing therapies. Scaffold-based tissue engineering emerges as a promising avenue for cartilage reconstitution. However, most scaffolds exhibit inadequate mechanical characteristics, poor biocompatibility, or absent cell adhesion sites. In this study, cartilage-like protein-polysaccharide hybrid hydrogel based on DOPA-modified hyaluronic acid, bovine type I collagen (Col I), and recombinant humanized type II collagen (rhCol II), denoted as HDCR. HDCR hydrogels possessed the advantage of injectability and in situ crosslinking through pH adjustment. Moreover, HDCR hydrogels exhibited a manipulable degradation rate and favorable biocompatibility. Notably, HDCR hydrogels significantly induced chondrogenic differentiation of rabbit bone marrow mesenchymal stem cells in vitro, as demonstrated by the upregulation of crucial chondrogenic genes (type II collagen, aggrecan) and the abundant accumulation of glycosaminoglycan. This approach presented a strategy to manufacture injectable, biodegradable scaffolds based on cartilage-like protein-polysaccharide polymers, offering a minimally invasive solution for cartilage repair.

Keywords Chondrogenic differentiation, Recombinant humanized collagen, Hyaluronic acid, Dopamine hydrochloride, Articular cartilage

*Correspondence:
Yafang Chen
yafang.chen@scu.edu.cn
Yujiang Fan
fan_yujiang@scu.edu.cn
Full list of author information is available at the end of the article

Graphical abstract

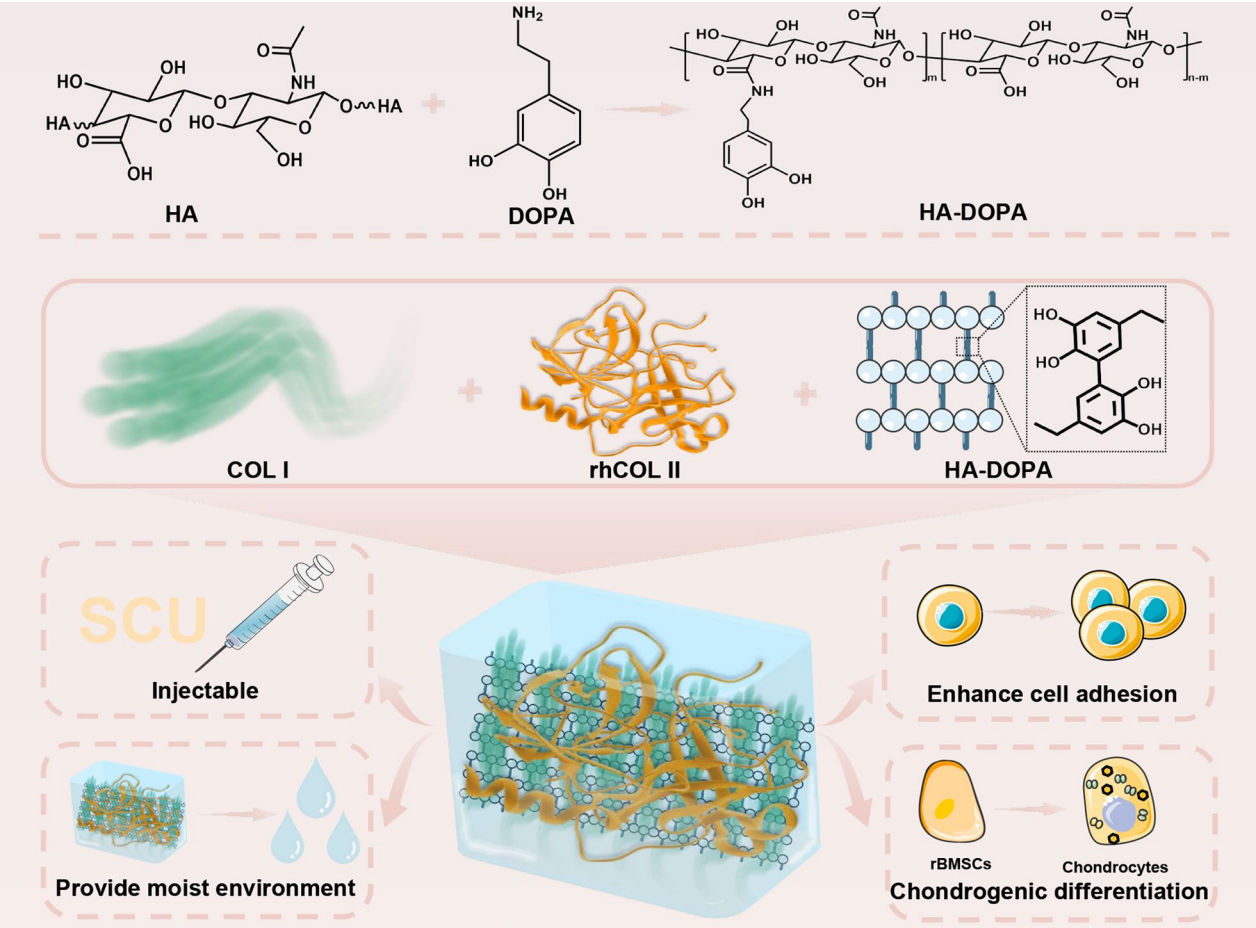

1 Introduction

Cartilage injury represents a significant societal and economic burden, given its high prevalence as a prevalent joint disorder [1]. The structure of cartilage tissue is devoid of blood vessels, nerves, and lymphatics, contributing to its restricted self-repair capacity following injury [2, 3]. Currently, commonly employed clinical approaches, such as autologous chondrocyte transplantation, osteochondral transplantation, and bone marrow stimulation, are encumbered by several inherent limitations, including heightened complications at the donor site, constrained availability, potential immunological reactions, and transmission of communicable diseases [4, 5]. Fortunately, the advent of tissue engineering technology, predicated on the modulation of scaffolds, growth factors, and cells, presents promising therapeutic strategies for cartilage repair [6, 7].

Hyaluronic acid (HA), the only non-sulfated glycosaminoglycan in cartilage, plays a pivotal role in both the extracellular matrix (ECM) and synovial fluid of cartilage [8, 9]. Notably, it exhibits the capability to augment lubrication performance at cartilage interfaces [10]. Nonetheless, the clinical utility of exogenous HA encounters challenges due to its rapid degradation, absence of cellular adhesion sites, and suboptimal mechanical properties, constraining its sustained efficacy for cartilage repair [11]. To tackle these issues, investigators have employed strategies such as the modification of hyaluronic acid (HA), for instance, by utilizing dopamine hydrochloride (DOPA), and so on [12]. The phenolic hydroxyl of DOPA contributed to enhancing adhesion, effectively facilitating binding to various materials or cell surfaces [13, 14]. Therefore, modifying hyaluronic acid or combining it with other materials can enhance its mechanical

properties, extending its degradation rate, and further increase cell adherence to the material [12, 15].

Type II collagen is traditionally acknowledged as an essential collagenous constituent within articular cartilage, exerting a pivotal role in the developmental and maturation processes of chondrocytes [16]. Consequently, there is a growing focus on type II collagen or materials derived from it in cartilage defect treatment and research [17]. Literature indicated that HA/Col II and Col I/Col II hydrogels had been employed to enhance the deposition of articular cartilage-specific matrix components through the loading of bone marrow mesenchymal stem cells (MSCs). Despite the hydrogel could be injected into the defect site, continued refinement was imperative to optimize the congruence between the geometry of scaffold and the anatomical contours of the cartilage defect site. [18]. However, the prevalent utilization of type II collagen derived from animals, such as pigs, cattle, and chickens, presents challenges including high cost, batch instability, immunogenicity, and the risk of transmitting infectious diseases [19, 20]. Consequently, recombinant humanized collagen II (rhCol II), generated through the cultivation of genetically modified microorganisms expressing human genes, emerges as an attractive alternative [21]. The rhCol II employed closely resembles human collagen in properties, offering potential advantages such as high purity, specific biological activity, batch stability, and lower immunogenicity [22]. Additionally, the addition of Col I has been proposed to play a crucial role in the mechanical stability of Col I/Col II hydrogels [18, 20]. Furthermore, an optimal ratio of Col I/II hybrid hydrogels has been reported to induce the differentiation of autologous MSCs into chondrocytes. Hydrogels containing both collagens exhibited higher glycosaminoglycan (GAG) yields compared to those containing only one type of collagen [23]. Our previous studies also demonstrated that Col I/HA hydrogels possessed appropriate mechanical properties, and the addition of HA prevented excessive collagen contraction, thereby playing a vital role in inducing stem cells to differentiate into chondrocytes [24]. Therefore, collagen-based hydrogels provide a biomimetic three-dimensional matrix microenvironment, presenting a promising strategy for repairing cartilage defects [25–28].

Inspired by the principles of bionics, this study was dedicated to investigating the effects of distinct groups of HDCR hydrogels on chondrogenic differentiation (Graphical abstract). The study commenced with the optimization of the material system to explore the performance characteristics of the various HDCR hydrogels. Subsequently, the biocompatibility of HDCR hydrogels was investigated in vitro. Finally, the study delved into assessing the efficacy of HDCR hydrogel in promoting chondrogenic differentiation of rBMSCs, employing histological staining, polymerase chain reaction (PCR), and quantification of glycosaminoglycan (GAG) levels in vitro.

2 Experimental section

2.1 Materials and methods

Hyaluronic acid (HA, Mw = 0.34 MDa) was purchased from Bloomage Freda Biopharma Corporation (Shandong, China). Type I collagen (Col I) was purchased from Tianjin ShijiKangtai Biomedical Engineering Corporation (Tianjin, China). Recombinant humanized type II collagen (rhCol II, Mw = 98.4 KDa, 1078 amino acids) was obtained from Jiangsu Trautec Medical Technology Co., Ltd (Jiangsu, Chain). 1-Ethyl-3-(3-dimethyllaminopropyl) carbodiimide hydrochloride (EDCI, 99%), N-hydroxysuccinimide (NHS, 99%), dopamine hydrochloride (DN, 99%) were provided by Best-reagent corporation (Chengdu, China). Hematoxylin and eosin staining (HE) were provided by Beijing Solarbio Science & Technology Co., Ltd (Beijing, China). DMEM medium (Hyclone) was purchased from Thermo Fisher Scientific Corporation (USA). Papain (sigma).

2.2 Preparation of HA-DOPA

HA-DOPA was prepared using the reported method [29]. Simply, 1 g of HA powder was added to 150 mL of ultra-pure water until a clear solution was obtained. The reaction took place under a vacuum atmosphere. Subsequently, EDC (2400 mg) and NHS (575 mg) were added. Then, the reaction proceeded for 1.5 h within a pH range of 4.75–5.0. Afterward, 1420 mg of DOPA was added, and the reaction pH was maintained at 4.75–5.0 for 24 h to obtain the HA-DOPA solution. The dialysis of the HA-DOPA solution was performed at pH 3.5 for three days. Finally, HA-DOPA was freeze-dried. The chemical composition was verified by ^{1}H-NMR (Bruker Amx-400, USA) and FTIR (Nicolet 6700, USA).

2.3 Fabrication of HDCR hydrogels

HA-DOPA was dissolved in DMEM medium (40 mg/mL), Col I was dissolved in ethanoic acid (0.5 M) to form a Col I solution at a concentration of 40 mg/mL, and rhCol II was dissolved in ultrapure water to form a rhCol II solution at a concentration of 80 mg/mL. Subsequently, appropriate volumes of these solutions were mixed (with final concentrations as shown in Table 1 and Additional file 1: Table S1), and 1 M NaOH solution was added to adjust the solution pH to 7.4. The resulting mixture was then injected into molds (8 mm * 3 mm), and HDCR hydrogels were obtained under 37 °C conditions (Table 2).

Table 1 The primary data of the experimental groups

Groups	HA-DOPA (mg/mL)	Col I (mg/mL)	rhCol II (mg/mL)
$HD_{15}C_{10}R_{10}$	15	10	10
$HD_{20}C_{10}R_{10}$	20	10	10
$HD_{20}C_{10}R_{0}$	20	10	0

Table 2 Primer sequences for GAPDH, Aggrecan, Col II, and Col I

Gene	Forward sequence primer	Reverse sequence primer
GAPDH	TCGGAGTGAACGGATTTGGC	TTCCCGTTCTCAGCCTTGAC
Aggrecan	GGCCACTGTTACCGTCACTT	GTCCTGAGCGTTGTTGTTGAC
Col II	TGATAAGGATGTGTGGAA GCCG	CAGGCAGTCCTTGGTGTCTTC
Col I	GTCGATGGCTGCACGAAAAA	GGGCCAACGTCCACATAGAA

2.4 Microstructure observation

HDCR hydrogels were freeze-dried using a critical point dryer (CPD, EMCPD300, Germany). The hydrogels underwent two rounds of sputtering and gold spraying. They were examined utilizing a Scanning Electron Microscope (Hitachi Limited, S-4800, Japan).

2.5 Rheological properties

We employed the TA Discovery DHR-2 rheometer (TA Instruments, USA) to measure the rheological property. The linear viscoelastic region was determined through a strain amplitude scan (a strain of 100–300%) [30].

2.6 Dynamic mechanical analysis (DMA)

The storage modulus and loss modulus of the hydrogels were determined using a dynamic mechanical analyzer (DMA, TA-Q800, USA) in multi-frequency mode with fixed frequencies of 1, 2, 5, and 10 Hz, and a preload force of 0.001 N. Each sample underwent three replicates for measurements.

2.7 Swelling ratio

Each HDCR hydrogel's dry weight (W_d) was weighed and immersed in phosphate buffered saline (PBS) solution, then placed in a shaker (37 °C) at 80 rpm. Finally, the hydrogels (W_s) were reweighed at specific time intervals until they reached swelling equilibrium.

$$\text{Swelling ratio} = (W_s - W_d)/W_d \times 100\%$$

2.8 Disintegration behavior

First, record the weight (W_o) of the hydrogel sample. After recording the weight, submerge the sample in ultra-pure water supplemented with 100 units of hyaluronidase per milliliter in a shaker at 37 °C. Then, they were taken out from the shaker at the indicated time points, the outer layer of water on the hydrogel was removed, and the hydrogel was reweighed (W_b).

$$\text{Degradation percentage} = (W_o - W_b)/W_o \times 100\%$$

2.9 The biocompatibility test and chondrogenic differentiation in vitro

rBMSCs ($1*10^4$ cells/well) were cultured in 24-well plates, co-cultivated with hydrogels, and subjected to cell viability assessments using the CCK-8 assay (Dojindo, Japan) and live/dead cell staining over a duration of 1, 3, and 7 days. In the CCK-8 experiment, the cells were incubated in a culture medium with CCK-8 (10%) for 2 h, following which the absorbance was measured. For the live/dead cell staining, the cells underwent incubation in a mixture containing fluorescein diacetate and propidium iodide for 3 min, and observation was conducted using confocal laser scanning microscopy (LSM 880; ZEISS).

rBMSCs ($1*10^4$ cells/well) were cultured in 24-well plates and co-cultured with three hydrogels for 14 days. Chondrogenic differentiation of rBMSCs was analyzed using hematoxylin eosin (HE) staining, toluidine blue (TB) staining, safranin O (SO) staining, and alcian blue (AB) staining.

The hydrogel/rBMSCs complex was prepared by adding cells ($5*10^6$ cells/mL) to the precursor solution as described in Sect. 2.3. GAG content was quantified and RNA expression was analyzed after 14 days culture. To measure the GAG content, the HDCR hydrogel/rBMSCs complex was collected in Eppendorf tubes with papain phosphate buffer and left to incubate overnight at a temperature of 65 °C. After centrifugation, the supernatant was collected, The Blyscan sGAG assay kit (B100, Biocolor) was used to determine the GAG content. The PicoGreen (dsDNA quantification reagent, enzyme) assay was employed to measure the DNA content. To analyze gene expression, RNA collection was fulfilled using the RNeasy Mini Kit (Qiagen). PCR detection was conducted using the SsoFast EvaGreen Supermix (Bio-rad) to assess the transcript levels of Col I, aggrecan (Agg), Col II, GAPDH. The transcript levels of other genes were determined relative to the GAPDH gene expression.

2.10 Histological analysis

After washing the rBMSCs one time with PBS, the samples were secured in 4% polyformaldehyde (w/v) for

48 h. HE, SO, TB, AB were used to analyze the chondrogenic differentiation in HDCR hydrogels. Positive cells staining was analyzed using image J.

2.11 Statistical analysis

All data were symbolized as the mean ± standard deviation (SD) of more than three independent tests. We conducted an analytical assessment using one-way analysis of variance (ANOVA). The data were examined using SPSS 22.0 software.

3 Results and discussion

3.1 Preparation and characterization of HA-DOPA

The depicted procedure for the preparation of HA-DOPA was illustrated in Fig. 1a. The carboxyl group of hyaluronic acid was activated under acidic conditions using EDCI and NHS, and then reacted with the amino and phenolic hydroxyl groups on an appropriate amount of DOPA to obtain HA-DOPA. Specifically, the C=O peak in HA was observed at 1441 cm^{-1}, while HA-DOPA exhibited specific absorption peaks at 1730 cm^{-1} in FTIR spectra, which were characteristic bands for superimposed amide or aromatic C=O [31], as depicted in Fig. 1b (black arrow). The structural characterization of the HA-DOPA was further confirmed by ^{1}H-NMR. As depicted in Fig. 1c, in contrast to the spectrum of HA, there were new peaks were observed at approximately 6.8 ppm, which were attributed to the characteristic catechol motifs based on previous reports [32]. Additionally, the peaks at 2.9 ppm, and 6.56–6.90 ppm were attributed to the methylene, and benzene groups in DOPA, respectively. Approximately 5% substitution degree of dopamine on HA, as determined based on the peak area ratio at 6.8 ppm in HA-DOPA to the peak area of the hydrogen atom at 1.9 ppm in HA. Collectively, the aforementioned results indicated that HA-DOPA was successfully synthesized.

3.2 Preparation and characterization of HDCR hydrogel

The macroscopic view of HDCR hydrogels was shown in Fig. 1d. The hydrogels were categorized into three groups, which was designated as $HD_{15}C_{10}R_{10}$, $HD_{20}C_{10}R_{10}$, and $HD_{20}C_{10}R_{0}$. As depicted in Fig. 1e, HDCR hydrogels were prepared according to the method described in Sect. 2.3, and the precursor solution transformed from a yellow liquid to a brown hydrogel at pH = 7.4, 37 °C, indicating the oxidation of DOPA. Previous studies have consistently shown that the adhesive properties of DOPA were primarily achieved through its oxidation process [33]. Meanwhile, the HDCR hydrogel could be easily injected with a 26 G syringe to form SCU shapes, suggesting excellent injectability and the ability to accurately fill irregular cartilage defects. Furthermore, the SEM analysis manifested that the HDCR hydrogels possessed a porose structure with uniform porosity (Fig. 1f). This finding confirmed that the HDCR hydrogels were beneficial for gas and nutrient exchange, which had been supported by previous research [29]. As depicted in Fig. 2a, the swelling ratio of $HD_{20}C_{10}R_{10}$ (129.93%) was higher than that of $HD_{15}C_{10}R_{10}$ (52.47%) and $HD_{20}C_{10}R_{0}$ (50.66%). Notably, all three groups of hydrogels achieved swelling stability within 24 h. The observed disparity in swelling behavior was attributed to the presence of DOPA, which possessed a catechol group. The oxygen atom in water established hydrogen bonds with the hydroxyl group of catechol, thereby facilitating the accumulation of water molecules within the DOPA-modified hyaluronic acid [34].

As depicted in Fig. 2b, the $HD_{20}C_{10}R_{0}$ hydrogel exhibited a rapid degradation rate during the initial stages, and the mass loss exceeded 90% at about 48 h. Conversely, $HD_{20}C_{10}R_{10}$ hydrogel and $HD_{15}C_{10}R_{10}$ hydrogel demonstrated smooth degradation in the presence of hyaluronidase solution, with complete disintegration exceeded 90% when the experiment was conducted for approximately 60 h. It has been reported that the enhancement of hydrogels against enzymatic degradation has been previously demonstrated through the crosslinking of hyaluronic acid with collagen amino groups [35]. The discrepancy of crosslinking degree was posited as a determinant influencing the disparate degradation rates observed among the three distinct hydrogel groups.

Moreover, the shear thinning behavior of the hydrogel was evaluated through viscosity measurement. As depicted in Fig. 2c, it was found that G' was dominant and gradually decreased under 100–200% strain, while G'' gradually increased, with a crossing point occurred at 200% strain. Beyond this strain, G'' became dominant, suggesting a transition of the hydrogel from a solid state to a liquid state due to the breaking of chemical bonds.

Additionally, the storage and loss modulus of all HDCR hydrogel were assessed using DMA. As presented in Fig. 2d–e, the loss modulus of HDCR hydrogels was in the range of approximately 0.1–1.3 kPa, and the storage modulus was in the range of approximately 0.3–2.5 kPa. It was noticed that both moduli increased with the rise in frequency (1–10 Hz) for all hydrogels. Notably, the $HD_{15}C_{10}R_{10}$ hydrogel and $HD_{20}C_{10}R_{10}$ hydrogel demonstrated higher values compared to $HD_{20}C_{10}R_{0}$ hydrogel, with the modulus of $HD_{15}C_{10}R_{10}$ hydrogel surpassing that of $HD_{20}C_{10}R_{10}$. It was plausible that rhCol II might exert a promotional effect on the modulus, thereby potentially contributing to the heightened moduli observed in $HD_{15}C_{10}R_{10}$ and $HD_{20}C_{10}R_{10}$ hydrogels in comparison to $HD_{20}C_{10}R_{0}$ hydrogel. The processes involve the oxidative cross-linking of phenolic hydroxyl groups in HA-DOPA and amino groups on Col I or rhCol II utilizing

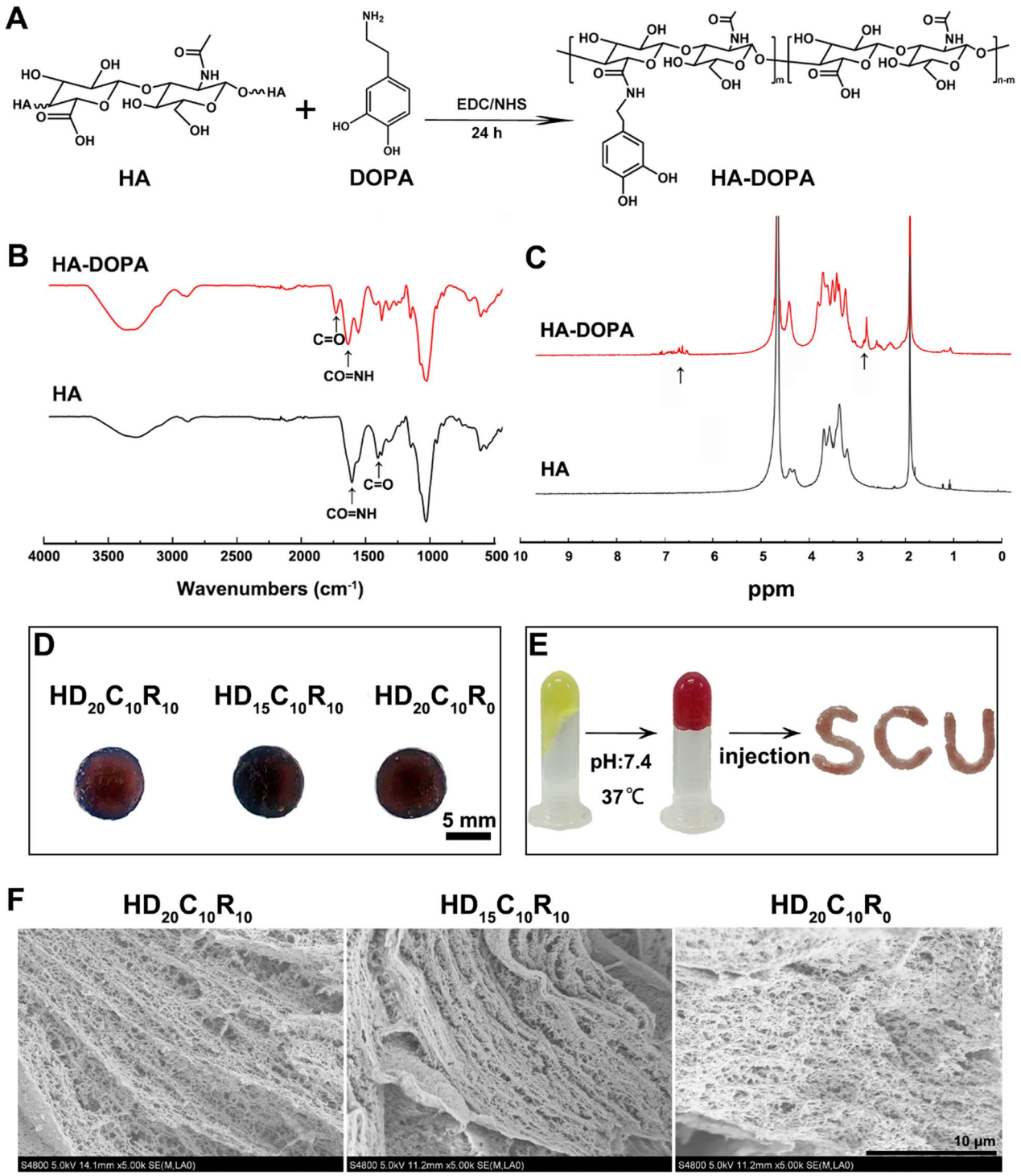

Fig. 1 **a** The synthesis route of HA-DOPA. **b** FTIR spectra of HA and HA-DOPA. **c** ^{1}H-NMR (D_2O) spectra of HA and HA-DOPA. **d** The macrostructure of hydrogels within different groups. **e** The gelation process and injection of HDCR hydrogels. **f** The microstructure (SEM) characterization of HDCR hydrogel

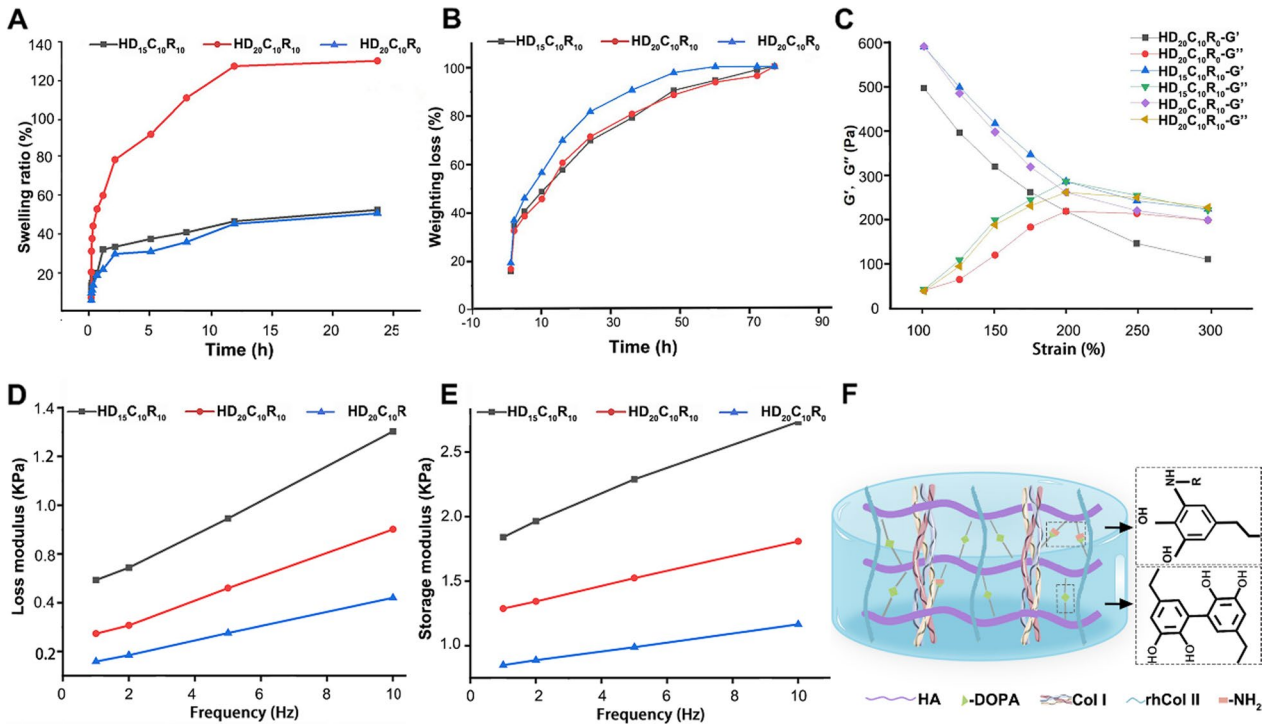

Fig. 2 **a** Swelling ratio of three groups of all hydrogels. **b** Disintegration behavior of all hydrogels in hyaluronidase environment. **c** The rheological test of all hydrogels by rheometer. **d** Loss modules of all hydrogels by DMA. **e** Storage modules of all hydrogels by DMA. **f** Self-crosslinking schematic diagram of HDCR hydrogel

the Michael addition reaction, as illustrated in Fig. 2f. The mechanical properties of hydrogels had a strong influence on cell growth and viability [36]. It was reported in the literature that at a modulus of about 200 Pa, the cell survival rate was more than 90%, while in the medium (about 100 Pa), the cell survival rate was about 80%. Another study also showed that DOPA-containing hydrogels with a modulus in the range of 1–3 kPa promoted cell proliferation. Together, this demonstrated that the mechanical properties of HDCR hydrogels play a promotional role in influencing cell growth and viability [29, 37].

3.3 In vitro proliferation and morphology of rBMSCs in HDCR hydrogels

Cell function and growth were tested using live/dead dyeing and CCK-8 assays to examine the impact of co-culturing rBMSCs with hydrogels. Originally, the investigation included $HD_{15}C_{10}R_{10}$, $HD_{20}C_{10}R_{10}$, $HD_{20}C_{10}R_0$, and $HD_{20}C_0R_{10}$. The results of the cell proliferation assay revealed significantly superior CCK-8 outcomes for $HD_{15}C_{10}R_{10}$ and $HD_{20}C_{10}R_{10}$ compared to $HD_{20}C_{10}R_0$ and $HD_{20}C_0R_{10}$ (Additional file 1: Fig. S1). Consequently, subsequent experimental groups were optimized, leading to the selection of $HD_{15}C_{10}R_{10}$, $HD_{20}C_{10}R_{10}$, and $HD_{20}C_{10}R_0$ for in-depth investigation. As depicted in Fig. 3a–b, all HDCR hydrogels exhibited an increase in viable cells count over time. Additionally, the morphology of rBMSCs within $HD_{20}C_{10}R_{10}$ hydrogel was further investigated using SEM (Fig. 3c). Remarkably, rBMSCs exhibited normal growth morphology within the pores of $HD_{20}C_{10}R_{10}$ hydrogel, indicating its conducive nature for cell growth and morphological maintenance. These findings collectively indicated that HDCR hydrogels in different groups were conducive to promoting the proliferation and maintaining the morphology of rBMSCs. Notably, $HD_{20}C_{10}R_{10}$ hydrogels emerged as the most effective in facilitating cell proliferation and adhesion.

3.4 Investigating the impact of HDCR hydrogel/rBMSCs complexes on chondrogenic differentiation

Histological staining was used to assess the cartilage differentiation in rBMSCs. Notably, the results of HE, SO, TB and AB staining (Fig. 4a) revealed that rBMSCs were $HD_{20}C_{10}R_{10}$ hydrogels exhibited more intense positive staining in comparison to the other hydrogels. Figure 4b–d illustrates that the densities of TB, SO, and AB positive cells were as follows: 71.34%, 76.86%, 55.02% in $HD_{20}C_{10}R_{10}$; 52.64%, 64.68%, 43.78% in $HD_{15}C_{10}R_{10}$; and 42.76%, 69.90%, 37.34% in $HD_{20}C_{10}R_0$. These

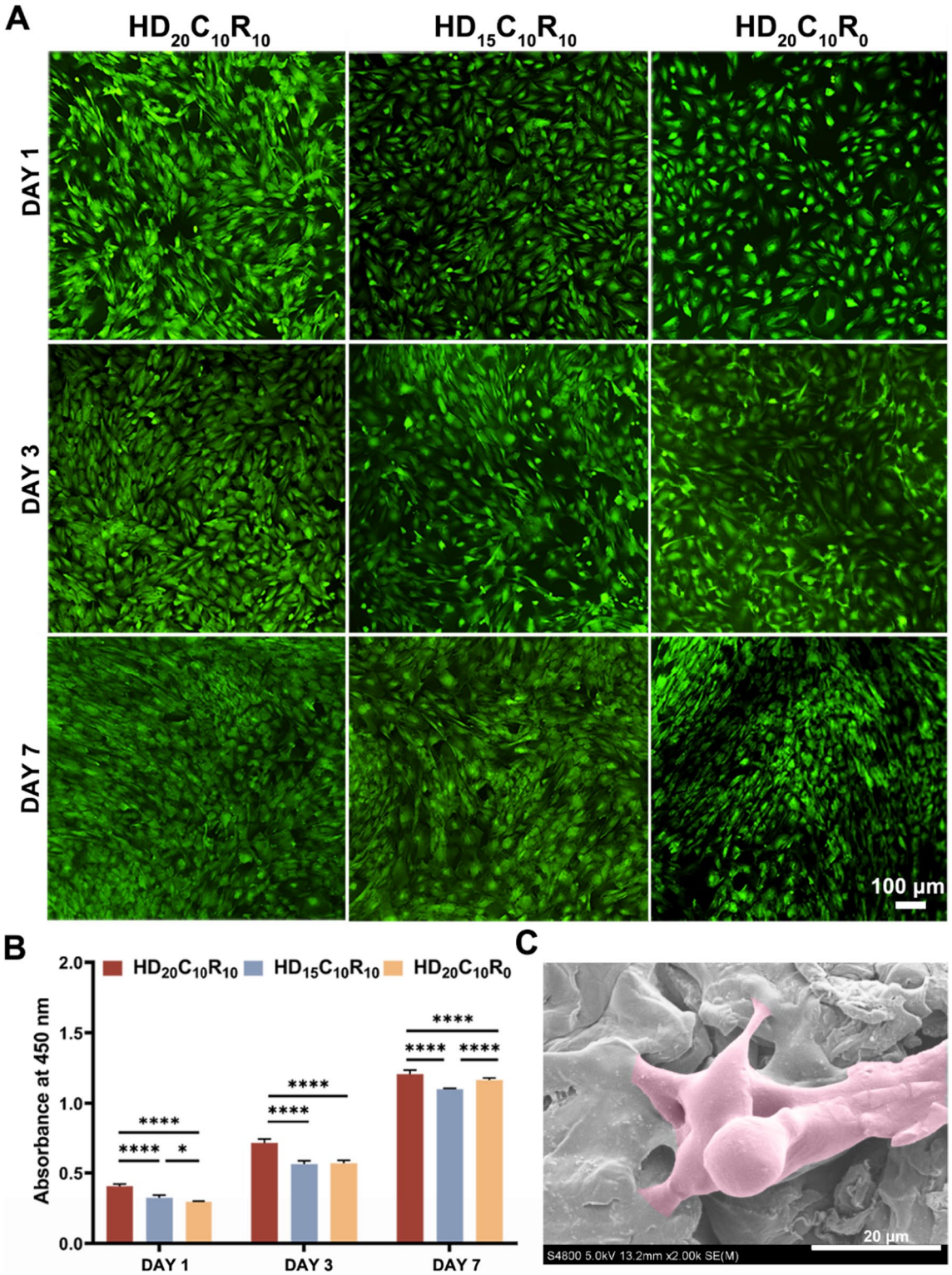

Fig. 3 **a** Representative fluorescence images for rBMSCs cultured within the hydrogels following incubation for 1, 3, and 7 days. **b** The proliferation of rBMSCs was quantified utilizing CCK-8 assay. **c** Morphological examination of rBMSCs within the $HD_{20}C_{10}R_{10}$ hydrogel was conducted on day 7 using SEM. $^{*}P < 0.05$, $^{****}P < 0.0001$

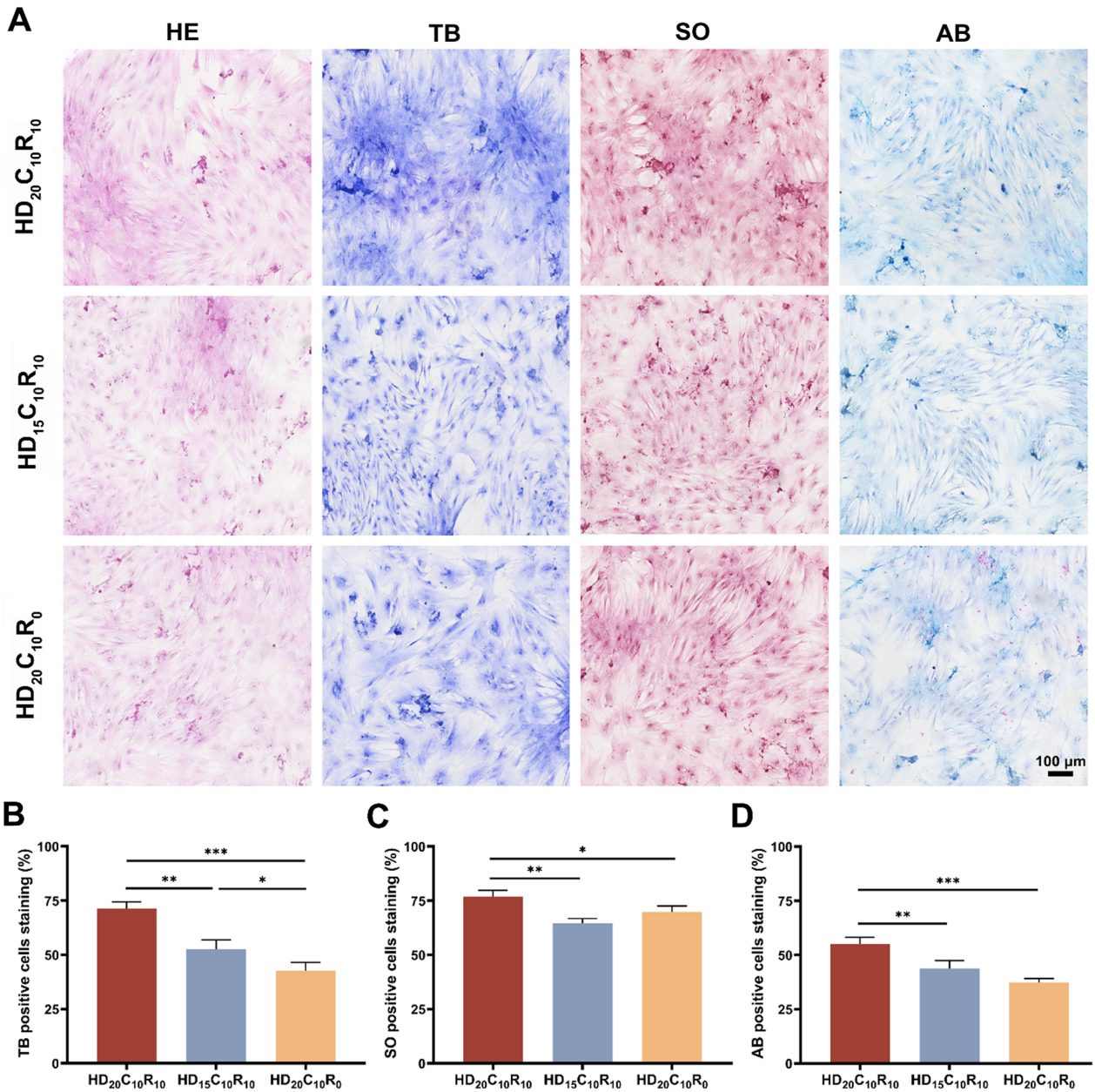

Fig. 4 **a** Histological staining of HE, TB, SO and AB for 14 days in vitro. **b** The staining ratio of TB positive cells. **c** The staining ratio of SO positive cells. **d** The staining ratio AB positive cells. *$P < 0.05$, **$P < 0.01$, ***$P < 0.001$, ****$P < 0.0001$

findings provided further supportive evidence for the augmented potential of chondrogenic differentiation in the $HD_{20}C_{10}R_{10}$ hydrogel, highlighting its superior performance in promoting chondrogenesis in rBMSCs.

Figure 5a presented the process of chondrogenic differentiation in vitro, while quantitative evaluation of chondrogenic related gene expression was performed using PCR. Figure 4b–d depicted the gene expression of collagen I (Col I), aggrecan (Agg), collagen II (Col II) in HDCR hydrogel/rBMSCs. Notably, the gene expression of Agg in $HD_{20}C_{10}R_{10}$ hydrogel was the highest compared to $HD_{15}C_{10}R_{10}$ hydrogel and $HD_{20}C_{10}R_0$ hydrogel after 14 days (Fig. 5c). Furthermore, the highest gene expression levels of Col II were observed in $HD_{20}C_{10}R_{10}$ hydrogel compared to $HD_{15}C_{10}R_{10}$ hydrogel and $HD_{20}C_{10}R_0$ hydrogel at 14 days (Fig. 5b). Conversely, $HD_{20}C_{10}R_0$ hydrogel exhibited higher Col I gene expression at 14 days (Fig. 5d), suggesting that the addition of rhCol II may have an inhibitory effect on chondrogenic fibrosis.

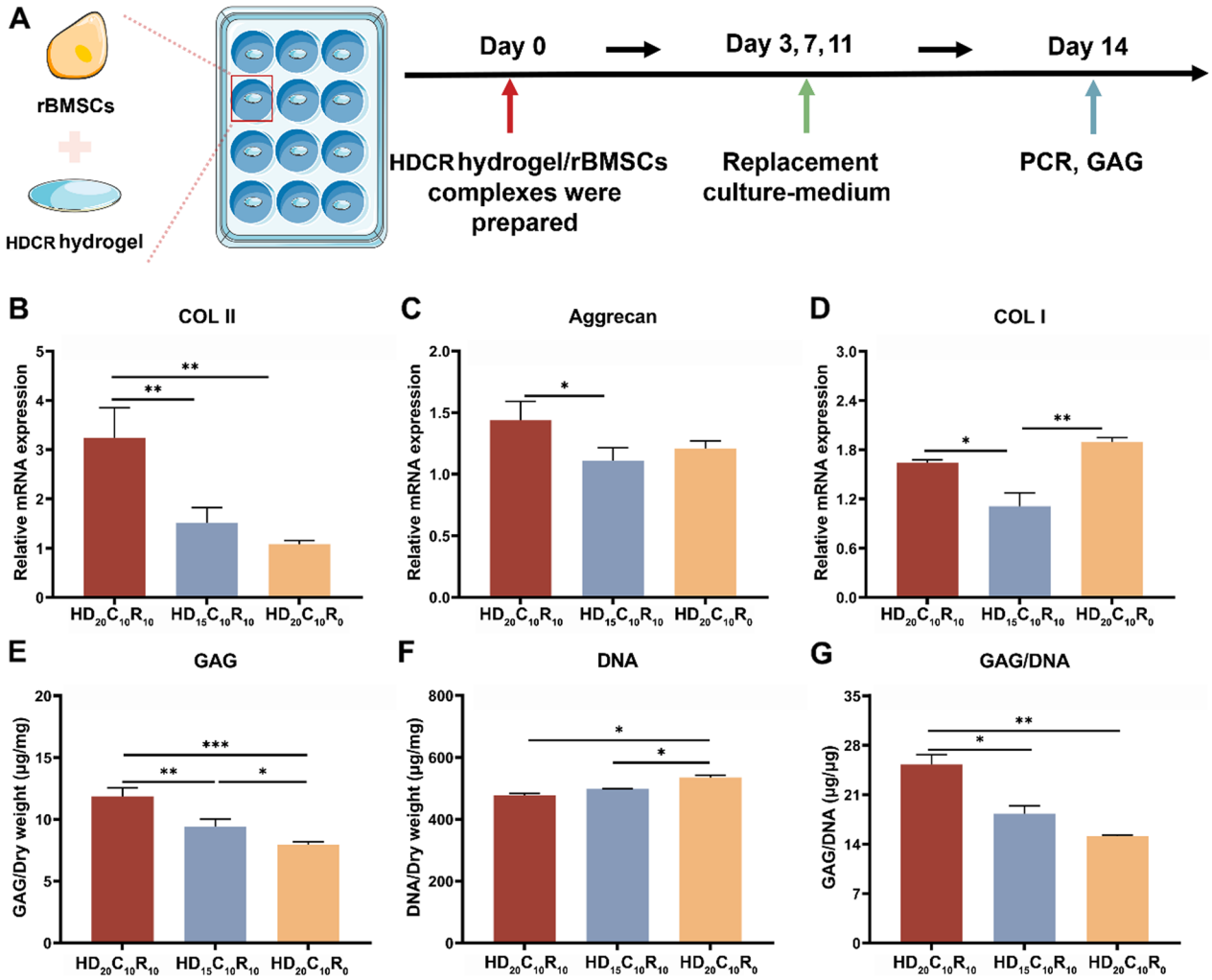

Fig. 5 **a** Diagram of chondrogenic differentiation of HDCR hydrogel/rBMSCs complexes in vitro. **b** Gene expression of Col II on day 14. **c** Gene expression of aggrecan on day 14. **d** Gene expression of Col I on day 14. **e** Quantification of GAGs produced by rBMSCs. **f** Quantification of DNA produced by rBMSCs. **g** GAG/DNA. $^{*}P < 0.05$, $^{**}P < 0.01$, $^{***}P < 0.001$

Furthermore, the quantification of glycosaminoglycan (GAG) content in the extracellular matrix of cartilage serves as a crucial determinant of chondrogenic differentiation in rBMSCs. As depicted in Fig. 5e–g, there was a sequential decline in glycosaminoglycan (GAG) content within the $HD_{20}C_{10}R_{10}$, $HD_{15}C_{10}R_{10}$, and $HD_{20}C_{10}R_{0}$. Conversely, DNA content exhibited an opposing trend. Notably, the GAG/DNA ratio in $HD_{20}C_{10}R_{10}$ hydrogel surpassed that in both the $HD_{15}C_{10}R_{10}$ and $HD_{20}C_{10}R_{0}$ hydrogels at 14 days, thereby corroborating the outcomes derived from PCR analysis. This finding emphasized the promising potential of $HD_{20}C_{10}R_{10}$ hydrogel in enhancing the chondrogenic lineage commitment of rBMSCs.

4 Conclusion

In summary, the objective of this study was to develop injectable and biodegradable cartilage-like protein-polysaccharide hybrid hydrogels. Among the various HDCR hydrogel groups, diverse mechanical characteristics and a controlled degradation rate were successfully attained. Additionally, HDCR hydrogels provided a suitable 3D microenvironment for rBMSCs, promoting cell survival and proliferation. More importantly, the favorable 3D microenvironment of HDCR hydrogels not only facilitated rBMSC adhesion but also significantly enhanced chondrogenic differentiation. Consequently, this investigation introduced a promising strategy for advancing the development of injectable and biodegradable scaffolds

based on protein-polysaccharide hybrids resembling cartilage, with implications for the field of cartilage tissue engineering.

Abbreviations

HDCR hydrogel	Dopamine-modified polysaccharide hybrid hydrogel
RhCol II	Recombinant humanized type II collagen
Col I	Bovine type I collagen
DOPA	Dopamine hydrochloride
HA	Hyaluronic acid
HA-DOPA	DOPA-modified hyaluronic acid
ECM	Extracellular matrix
rBMSCs	Rabbit bone marrow mesenchymal stem cells
GAG	Glycosaminoglycan
SEM	Scanning electron microscope
Agg	Aggrecan
HE	Hematoxylin eosin
SO	Safranin O
AB	Alcian blue
TB	Toluidine blue

Supplementary Information

The online version contains supplementary material available at https://doi.org/10.1186/s42825-023-00146-2.

Additional file 1. **Table S1.** The primary data of the experimental groups. **Figure S1.** rBMSCs proliferation measured by CCK-8 kit.

Acknowledgements
The authors thank Dr. Guolong Meng and Dr. Jiao Lu (National Engineering Research Center for Biomaterials, Sichuan University) for their help in the characterization of SEM and CLSM.

Author contributions
XYZ designed this project and revised the manuscript. XYZ and HJC and CXL performed experiments, analyzed data and wrote the manuscript. XZ and CH and ZQD and performed experiments and draw the scheme. YFC and JL and XDZ and YJF reviewed the manuscript. All authors read and approved the final manuscript. All the authors discussed the results and finalized the manuscript.

Funding
This work was supported by the National Key Research and Development Program of China (Grant No. 2022YFC2401800) and Fundamental Research Funds for the Central Universities (2022SCU12104) and the National Natural Science Foundation of China (Grant No. 51973136) and Sichuan University postdoctoral interdisciplinary Innovation Fund.

Availability of data and materials
All data generated or analyzed during this study are included in this published article.

Declarations

Ethics approval and consent to participate
Not applicable.

Consent for publication
Not applicable.

Competing interests
The authors declare that they have no competing interests.

Author details
[1]National Engineering Research Center for Biomaterials, Sichuan University, 29# Wangjiang Road, Chengdu 610064, China. [2]College of Biomedical Engineering, Sichuan University, 29# Wangjiang Road, Chengdu 610064, China. [3]Collaborative Innovation Centre of Regenerative Medicine and Medical BioResource Development and Application Co-constructed By the Province and Ministry, Guangxi Medical University, Nanning 530021, Guangxi, China. [4]Sichuan Testing Center for Biomaterials and Medical Devices, Chengdu 610064, China.

Received: 2 September 2023 Revised: 16 December 2023 Accepted: 28 December 2023
Published online: 08 January 2024

References

1. Arden NK, Perry TA, Bannuru RR, Bruyère O, Cooper C, Haugen IK, et al. Non-surgical management of knee osteoarthritis: comparison of ESCEO and OARSI 2019 guidelines. Nat Rev Rheumatol. 2021;17(1):59–66.
2. Tuli R, Li W-J, Tuan RS. Current state of cartilage tissue engineering. Arthritis Res Ther. 2003;5(5):1–4.
3. Armiento AR, Alini M, Stoddart MJ. Articular fibrocartilage—why does hyaline cartilage fail to repair? Adv Drug Deliv Rev. 2019;146:289–305.
4. Sarzaeem MM, Razi M, Kazemian G, Moghaddam ME, Rasi AM, Karimi M. Comparing efficacy of three methods of tranexamic acid administration in reducing hemoglobin drop following total knee arthroplasty. J Arthroplast. 2014;29(8):1521–4.
5. Wang Z, Le H, Wang Y, Liu H, Li Z, Yang X, et al. Instructive cartilage regeneration modalities with advanced therapeutic implantations under abnormal conditions. Bioact Mater. 2022;11:317–38.
6. Koons GL, Diba M, Mikos AG. Materials design for bone-tissue engineering. Nat Rev Mater. 2020;5(8):584–603.
7. Chen FH, Rousche KT, Tuan RS. Technology insight: adult stem cells in cartilage regeneration and tissue engineering. Nat Clin Pract Rheumatol. 2006;2(7):373–82.
8. Schuurmans CCL, Mihajlovic M, Hiemstra C, et al. Hyaluronic acid and chondroitin sulfate (meth) acrylate-based hydrogels for tissue engineering: synthesis, characteristics and pre-clinical evaluation. Biomaterials. 2021;268:120602.
9. Wei W, Ma Y, Yao X, Zhou W, Wang X, Li C, et al. Advanced hydrogels for the repair of cartilage defects and regeneration. Bioact Mater. 2021;6(4):998–1011.
10. Lin WF, Liu Z, Kampf N, Klein J. The role of hyaluronic acid in cartilage boundary lubrication. Cells. 2020;9(7):1606.
11. Wolf KJ, Kumar S. Hyaluronic acid: incorporating the bio into the material. ACS Biomater Sci Eng. 2019;5(8):3753–65.
12. Zhou D, Li S, Pei M, Yang H, Gu S, Tao Y, et al. Dopamine-modified hyaluronic acid hydrogel adhesives with fast-forming and high tissue adhesion. ACS Appl Mater Interfaces. 2020;12(16):18225–34.
13. Faure E, Falentin-Daudré C, Jérôme C, Lyskawa J, Fournier D, Woisel P, et al. Catechols as versatile platforms in polymer chemistry. Prog Polym Sci. 2013;38(1):236–70.
14. Rodriguez-Emmenegger C, Preuss CM, Yameen B, Pop-Georgievski O, Bachmann M, Mueller JO, et al. Controlled cell adhesion on poly(dopamine) interfaces photopatterned with non-fouling brushes. Adv Mater. 2013;25(42):6123–7.
15. Dovedytis M, Liu ZJ, Bartlett SJER. Hyaluronic acid and its biomedical applications: a review. Eng Regener. 2020;1:102–13.
16. Zhu J, Li Z, Zou Y, Lu G, Ronca A, D'Amora U, et al. Advanced application of collagen-based biomaterials in tissue repair and restoration. J Leather Sci Eng. 2022;4(1):30.
17. Lazarini M, Bordeaux-Rego P, Giardini-Rosa R, et al. Natural type II collagen hydrogel, fibrin sealant, and adipose-derived stem cells as a promising combination for articular cartilage repair. Cartilage. 2017;8(4):439.
18. O'Shea DG, Hodgkinson T, Curtin CM, et al. An injectable and 3D printable pro-chondrogenic hyaluronic acid and collagen type II composite hydrogel for the repair of articular cartilage defects. Biofabrication. 2023;16(1):015007.
19. Wang J, Hu H, Wang J, Qiu H, Gao Y, Xu Y, et al. Characterization of recombinant humanized collagen type III and its influence on cell behavior and phenotype. J Leather Sci Eng. 2022;4(1):33.

20. Bonnet C, Charriere G, Vaquier J, Bertin P, Vergne P, Treves R. Bovine collagen induced systemic symptoms: antibody formation against bovine and human collagen. J Rheumatol. 1996;23(3):545–7.
21. Báez J, Olsen D, Polarek JW. Recombinant microbial systems for the production of human collagen and gelatin. Appl Microbiol Biotechnol. 2005;69(3):245–52.
22. Yang Y, Campbell Ritchie A, Everitt NM. Recombinant human collagen/chitosan-based soft hydrogels as biomaterials for soft tissue engineering. Mater Sci Eng C. 2021;121:111846.
23. Kilmer CE, Battistoni CM, Cox A, Breur GJ, Panitch A, Liu JC. Collagen type I and II blend hydrogel with autologous mesenchymal stem cells as a scaffold for articular cartilage defect repair. ACS Biomater Sci Eng. 2020;6(6):3464–76.
24. Chen Y, Sui J, Wang Q, Yin Y, Liu J, Wang Q, et al. Injectable self-crosslinking HA-SH/Col I blend hydrogels for in vitro construction of engineered cartilage. Carbohyd Polym. 2018;190:57–66.
25. Liu J, Yu C, Chen Y, Cai H, Lin H, Sun Y, et al. Fast fabrication of stable cartilage-like tissue using collagen hydrogel microsphere culture. J Mater Chem B. 2017;5(46):9130–40.
26. Li YY, Choy TH, Ho FC, Chan PB. Scaffold composition affects cytoskeleton organization, cell–matrix interaction and the cellular fate of human mesenchymal stem cells upon chondrogenic differentiation. Biomaterials. 2015;52:208–20.
27. Zhang D, Wu X, Chen J, Lin K. The development of collagen based composite scaffolds for bone regeneration. Bioact Mater. 2018;3(1):129–38.
28. Chen Q, Pei Y, Tang K, Albu-Kaya MG. Structure, extraction, processing, and applications of collagen as an ideal component for biomaterials—a review. Collagen Leather. 2023;5(1):20.
29. Li Z, Cao H, Xu Y, Li X, Han X, Fan Y, et al. Bioinspired polysaccharide hybrid hydrogel promoted recruitment and chondrogenic differentiation of bone marrow mesenchymal stem cells. Carbohydr Polym. 2021;267:118224.
30. Du W, Tan L, Zhang Y, Yang H, Chen H. Dynamic rheological investigation during curing of a thermoset polythiourethane system. Int J Polym Sci. 2019;2019:8452793.
31. Cheng H, Shi Z, Yue K, Huang X, Xu Y, Gao C, et al. Sprayable hydrogel dressing accelerates wound healing with combined reactive oxygen species-scavenging and antibacterial abilities. Acta Biomater. 2021;124:219–32.
32. Miller R, Kim Y, Park CG, Torres C, Kim B, Lee J, et al. Extending the bioavailability of hydrophilic antioxidants for metal ion detoxification via crystallization with polysaccharide dopamine. ACS Appl Mater Interfaces. 2022;14(35):39759–74.
33. Salzlechner C, Haghighi T, Huebscher I, Walther AR, Schell S, Gardner A, et al. Adhesive hydrogels for maxillofacial tissue regeneration using minimally invasive procedures. Adv Healthc Mater. 2020;9(4):1901134.
34. Neto AI, Cibrão AC, Correia CR, Carvalho RR, Luz GM, Ferrer GG, et al. Nanostructured polymeric coatings based on chitosan and dopamine-modified hyaluronic acid for biomedical applications. Small. 2014;10(12):2459–69.
35. Gautieri A, Redaelli A, Buehler MJ, Vesentini S. Age- and diabetes-related nonenzymatic crosslinks in collagen fibrils: candidate amino acids involved in advanced glycation end-products. Matrix Biol. 2014;34:89–95.
36. Gao Y, Liu Q, Kong W, Wang J, He L, Guo L, et al. Activated hyaluronic acid/collagen composite hydrogel with tunable physical properties and improved biological properties. Int J Biol Macromol. 2020;164:2186–96.
37. Kim IG, Gil CH, Seo J, Park SJ, Subbiah R, Jung TH, Kim JS, Jeong YH, Chung HM, Lee JH, Lee MR, Moon SH, Park K. Mechanotransduction of human pluripotent stem cells cultivated on tunable cell-derived extracellular matrix. Biomaterials. 2018;150:100–11.

Publisher's Note